This article has been accepted for publication in IEEE Transactions on Automatic Control. This is the author's version which has not been fully edited and content may change prior to final publication. Citation information: DOI 10.1109/TAC.2022.3230764

Finite-dimensional characterisation of optimal control laws over an infinite horizon for nonlinear systems

M. Sassano, *Senior Member, IEEE* and T. Mylvaganam, *Senior Member, IEEE*

***Abstract*— Infinite-horizon optimal control problems for nonlinear systems are considered. Due to the nonlinear and intrinsically *infinite-dimensional* nature of the task, solving such optimal control problems is challenging. In this paper an *exact finite-dimensional* characterisation of the optimal solution over the entire horizon is proposed. This is obtained via the (static) minimisation of a suitably defined function of (projected) trajectories of the underlying Hamiltonian dynamics on a hypersphere of fixed radius. The result is achieved in the spirit of the so-called *shooting methods* by introducing, via simultaneous forward/backward propagation, an *intermediate shooting point* much closer to the origin, regardless of the actual initial state. A modified strategy allows one to determine an arbitrarily accurate approximate solution by means of standard gradient-descent algorithms over compact domains. Finally, to further increase robustness of the control law, a receding-horizon architecture is envisioned by designing a sequence of shrinking hyperspheres. These aspects are illustrated by means of a benchmark numerical simulation.**

***Index Terms*— Optimal Control; Nonlinear Systems; Hamiltonian systems; Stability of NL systems.**

I. Introduction

Infinite-horizon optimal control problems for nonlinear systems are considered herein. The class of problems involves determining feedback stabilising control policies with the property that a certain cost functional is minimised along the trajectories of the resulting closed-loop system (see for instance [1]). Such problems are, in general, challenging nonconvex, infinite-dimensional optimisation problems. The optimal policy can be determined by relying either on Pontryagin's Minimum Principle (PMP) [2] or on the Dynamic Programming (DP) method [3], [4]. A combination of the two methods may also be viable [5], [6], [7], [8]. In practice both approaches possess specific drawbacks. The former implies that the optimal trajectory satisfies a certain ordinary differential equation, defined on an extended state-space with the initial condition partially *unknown*. The latter, on the other hand, relies on the solution of a partial differential equation (PDE), namely the Hamilton-Jacobi-Bellman (HJB) equation, for which closed-form solutions are rarely feasible to obtain and for which numerical solutions also pose a significant challenge due to the computational complexity associated with solving nonlinear PDEs numerically. Various approaches have been explored to overcome the computational hurdles associated with solving both finite and infinite-horizon optimal control problems, encompassing numerical methods [9], approaches based on the notion of *viscosity solution* [10], [11] or regional methods [12], to mention just a few. For the special case in which the dynamics are linear and the running cost is quadratic in the input and state, namely the well-known Linear Quadratic Regulator (LQR), solutions are readily found via the Algebraic Riccati Equation (ARE). Consequently, methods based on state-dependent Riccati equations (SDREs) have emerged for nonlinear problems, where essentially an ARE is solved pointwise along the trajectory of the system. While the approach is *relatively* simple from a computational point of view, the resulting control strategies are, in general, suboptimal and characterised by a quality of approximation that is not easily quantifiable *a priori* (see, e.g., [13] and references therein). In [14], [15] the solution of a single algebraic matrix equation is used to construct a *dynamic* control law which satisfies, by construction, a partial differential inequality in some non-empty neighbourhood including an equilibrium of the system. Consequently, the approach solves (exactly) a modified optimal control problem and yields an approximate (local) solution of the original optimal control problem, where the *level of approximation* can be explicitly quantified. Alternative approaches to obtain approximate solutions analytically can be found, for instance, in [16]. Therein, the HJB PDE is considered and, recognising the relevance of a certain associated Hamiltonian system (which possesses a stable invariant manifold characterising the solution of the HJB PDE), two approaches for obtaining approximate solutions are proposed. One approach relies on viewing the control input as a Hamiltonian perturbation and uses geometric tools to approximate the stable manifold associated with the aforementioned Hamiltonian system. Methods to compute invariant manifolds of dynamical systems are also relevant in this regard (see, *e.g.* [17], [18]). The second approach relies on expressing the dynamics of a system in terms of a linear and a nonlinear component and presents a sequence which provides an approximation of the flow of the Hamiltonian system on the stable manifold. A different approach, still utilising the relationship between optimal control problems and their associated Hamiltonian systems, is taken in [19]. Therein, solutions for the LQR problem with input constraints

M. Sassano is with Dipartimento di Ingegneria Civile ed Ingegneria Informatica, Università di Roma Tor Vergata, 00133 Roma, Italy.

T. Mylvaganam is with the Department of Aeronautics, Imperial College London, London SW7 2AZ, UK.

This work is licensed under a Creative Commons Attribution 4.0 License. For more information, see https://creativecommons.org/licenses/by/4.0/

This article has been accepted for publication in IEEE Transactions on Automatic Control. This is the author's version which has not been fully edited and content may change prior to final publication. Citation information: DOI 10.1109/TAC.2022.3230764

are solved via a numerical procedure which exploits the property that the optimal solution is associated with a specific trajectory of the associated Hamiltonian system. Approximate solutions to the constrained optimal control problems are then found via the generation of a "lookup table" created based on backwards integration of the Hamiltonian dynamics from initial conditions in a neighborhood of the origin. Similarly to the approaches presented in [16], [19], we utilise the Hamiltonian system associated with an optimal control problem to characterise exact and approximate solutions of the problem. Differently from the results in [16], [19], however, the approach proposed herein ultimately requires only the solution of an (unconstrained) static optimisation problem. It does not rely on approximating the stable invariant manifold of the Hamiltonian system and does not require any sequential process or lookup table. The Hamiltonian dynamics are in fact employed to design a certain finite-dimensional cost function that attains its minimal value at the intersecting point of the optimal trajectory and a hypersphere of fixed radius.

To be more specific, in this paper we consider a class of infinite-horizon optimal control problems characterised by the property that the underlying value function satisfies a certain differentiability condition. This condition is implied (locally) by equivalent properties of the data of the problem and, hence, is easily verifiable *a priori* (see [20]). Such differentiability conditions are instrumental in showing that a solution to the HJB PDE also satisfies the so-called Hamilton condition (*sensitivity relations*, see *e.g.* [21]) associated with Pontryagin's Minimum Principle. Namely, the optimal process is associated with a certain trajectory of the Hamiltonian system defined on the extended state/costate space, obtained via a Hamiltonian lifting (see, e.g. [16]). We utilise the above property to provide a finite-dimensional characterisation of the solution of the problem via the formulation of a static minimisation problem, defined in terms of trajectories of the underlying Hamiltonian system. More precisely, the solution of the optimal control problem is determined by first computing the intersection of the corresponding trajectory of the Hamiltonian system with a sufficiently small hypersphere around the origin. Consequently, the optimal process is determined by *forward* and *backward* propagating the flow of the Hamiltonian dynamics from this *intermediate point*, which is a minimiser of the aforementioned *static* cost function, involving the initial condition of the underlying plant. It is worth observing that, differently from existing methods that aim at providing a finite-dimensional characterisation of the optimal policy, herein the results do not rely on any quantisation arguments with respect to time or space. The proposed conditions instead provide an *exact finite-dimensional description of the entire optimal trajectory*, namely over the infinite horizon. In practice the static minimisation problem cannot, in general, be solved by using standard gradient-descent algorithms unless explicit expressions for the flow of the Hamiltonian dynamics and its sensitivity are available. Such expressions are rarely available except for specially structured classes of systems, such as for linear systems. This limitation is therefore circumvented through the introduction of a hybrid architecture that comprises state variables whose evolution captures the propagation of the flow of the Hamiltonian dynamics and of its sensitivity to the initial condition. Finally, a receding-horizon implementation of the architecture is suggested by suitably generating a sequence of hyperspheres of decreasing radii. Building on the property that such a strategy provides not only a sub-optimal policy over a restricted time interval but ideally the entire (infinite-horizon) optimal policy, the novel algorithm allows for particularly large moving windows without hindering the accuracy of the overall scheme. This is an interesting difference with respect to existing receding-horizon strategies that are based on the computation of a (relatively small) portion of the optimal strategy at each sampling instant.

The remainder of the paper is organised as follows. The infinite-horizon optimal control problem and some preliminaries are recalled in Section II. A finite-dimensional characterisation of optimal control laws is provided in Section III. Two results are provided therein: one is the characterisation of the stable (which yields the optimal control law) and the unstable invariant submanifolds of the underlying Hamiltonian system via a static minimisation problem. Through this problem the set containing the intersections between the invariant manifolds and a hyphersphere of fixed radius is determined. Having determined these intersection points, the optimal control input can be readily obtained by backwards/forwards integration of the flow of the Hamiltonian system. A companion result yields a characterisation of trajectories "close" to the stable and unstable submanifolds via a modified (saturated) static minimisation problem. The latter lends itself efficiently to an algorithmic interpretation, which is provided in Section IV. Note that while the stable and unstable manifolds of the Hamiltonian system are crucial in the characterisation of the optimal control laws, the proposed approach does not require determining the submanifolds themselves. Namely, the relationship between the Hamiltonian system, its stable/unstable invariant manifolds and the optimal control law is exploited to determine the *specific* trajectory of the Hamiltonian system associated with the optimal control input (for a given initial condition) of an infinite-horizon optimal control problem. Finally, the results presented in this paper are demonstrated by means of a benchmark example, before some concluding remarks are provided in Sections V and VI, respectively.

Notation. Let $\bar{\mathbb{R}}$ denote the extended real number line, namely $\bar{\mathbb{R}} = \mathbb{R} \cup \{-\infty, +\infty\}$. Given two vectors $x_1 \in \mathbb{R}^{n_1}$ and $x_2 \in \mathbb{R}^{n_2}$, (x_1, x_2) denotes the column stack of x_1 and x_2, *i.e.* $(x_1, x_2) := [x_1^\top, x_2^\top]^\top \in \mathbb{R}^{n_1+n_2}$. $C^\kappa(D)$ denotes the set of functions defined over D with continuous derivatives of order κ. Considering a function $f : \mathbb{R}^n \to \mathbb{R}^m$, $f \in C^1(\mathbb{R}^n)$, we let $\nabla f = \left[(\partial f/\partial x_1)^\top, ..., (\partial f/\partial x_n)^\top\right]^\top$ denote the Jacobian matrix of $f(x)$, with respect to $x = [x_1, ..., x_n]^\top \in \mathbb{R}^n$. When f is a scalar function, $\nabla f = [\partial f/\partial x_1, ..., \partial f/\partial x_n]^\top$ denotes the *column* vector of partial derivatives of f with respect to x, whereas $\nabla^2 f$ denotes its Hessian matrix. Given a square matrix M, $\sigma(M)$ denotes its spectrum.

II. Problem formulation and preliminaries

Consider a dynamical system with state $x : \mathbb{R} \to \mathbb{R}^n$ and control input $u : \mathbb{R} \to \mathbb{R}^m$. In this paper we consider the infinite-horizon optimal control problem recalled below.

This work is licensed under a Creative Commons Attribution 4.0 License. For more information, see https://creativecommons.org/licenses/by/4.0/

This article has been accepted for publication in IEEE Transactions on Automatic Control. This is the author's version which has not been fully edited and content may change prior to final publication. Citation information: DOI 10.1109/TAC.2022.3230764

Problem 1. Determine, if it exists, a continuous function $u^\star : C^0(\mathbb{R}_{\geqslant 0}) \to \mathbb{R}^m$ that solves the dynamic optimisation problem $\mathcal{Q}_{x_0}$ defined as

$$\min_u \left\{ \frac{1}{2} \int_0^\infty (q(x(t)) + \|u(t)\|^2) dt \right\}, \tag{1a}$$

$$\dot{x} = f(x) + g(x)u, \quad x(0) = x_0\,, \tag{1b}$$

for any $x_0 \in \mathcal{X}$, where $\mathcal{X}$ is a non-empty neighbourhood of the origin and where the positive definite function $q : \mathbb{R}^n \to \mathbb{R}_{>0}$, the vector field $f : \mathbb{R}^n \to \mathbb{R}^n$, $f(0) = 0$, and and the vector fields $g_i : \mathbb{R}^n \to \mathbb{R}^n$, $i = 1, ..., m$, columns of g, are assumed to be sufficiently smooth functions in $\mathcal{X}$[1]. ∘

The first term of (1a) quantifies a running cost on the state variable while the second term represents a penalty on the control effort. The overall integral in (1a) is the cost functional to be minimised via the selection of the control input u, whereas the constraints (1b) represent the dynamics dictating the behaviour of the system and the initial condition of the state of the system. Problem 1 is associated with a so-called *value function* $V^\star : \mathcal{X} \to \mathbb{R}_{>0}$, defined as $V^\star(x_0) \triangleq \min_u\{\mathcal{Q}_{x_0}\}$, for any initial condition $x_0 \in \mathcal{X}$ (see, for instance, [21]).

Remark 1. It has been shown in [20] that $V^\star$ locally inherits certain properties from the problem data. In particular, provided the requirements of Problem 1 hold, there exists a neighbourhood $\mathcal{X}$ of the origin such that $V^\star \in C^2(\mathcal{X})$. ▲

Let $A := \nabla f|_{x=0}$ and $B = g(0)$ describe the *linearized dynamics*, $\delta\dot{x} = A\delta x + Bu$, of (1b) around the origin and let $\bar{q}(x) = x^\top Q x$, with $Q := \nabla^2 q(x)|_{x=0}$ represent the corresponding quadratic approximation of the running cost. The following assumption is instrumental for guaranteeing the existence of a solution to Problem 1, at least locally around the origin, as well as ensuring (local) asymptotic stability of the origin for the closed-loop optimal system.

Assumption 1. The pairs (A, B) and (A, Q) are stabilizable and observable, respectively. ∘

Note that, as a consequence of Assumption 1, the linearized dynamics together with the quadratic approximation of the running cost admit the optimal solution $u_\ell = -B^\top P x$, where $P \in \mathbb{R}^{n\times n}$ denotes the (unique) positive definite solution of the Algebraic Riccati Equation (ARE)

$$0 = A^\top P + PA + Q - PBB^\top P\,. \tag{2}$$

It can be demonstrated by means of the DP approach (see *e.g.* [23]) that the solution of Problem 1 is given by the feedback control law

$$u^\star(x) = -g(x)^\top \nabla V(x)\,, \tag{3}$$

provided $V : \mathcal{X} \to \mathbb{R}_{>0}$, $V(0) = 0$, $V \in C^\kappa(\mathcal{X})$ with $\kappa \geqslant 1$, is a solution to the PDE

$$0 = \frac{1}{2}q(x) + \nabla V(x)^\top f(x) - \frac{1}{2}\nabla V(x)^\top g(x) g(x)^\top \nabla V(x)\,, \tag{4}$$

[1]The smoothness assumption on the data of the problem is a condition verifiable *a priori*, see *e.g.* [22], [20].

for any $x \in \mathcal{X}$, with $\mathcal{X}$ a neighbourhood of the origin. In particular, (4) is derived from the HJB PDE

$$0 = \min_u \left\{ \frac{1}{2}q(x) + \frac{1}{2}u^\top u + \nabla V(x)^\top (f(x) + g(x)u) \right\}, \tag{5}$$

for any $x \in \mathcal{X}$. Moreover, such function V coincides with the value function $V^\star$, which possesses the properties mentioned in Remark 1. The DP approach provides sufficient conditions for optimality: a function V satisfying the HJB PDE (4) yields, via (3), a solution to the optimal control problem $\mathcal{Q}_{x_0}$ in (1) in terms of a feedback control.

Since DP provides the optimal solution in terms of a feedback policy, the DP approach yields (locally) information regarding the optimal solution and the minimal cost for *any* initial condition, hence slightly generalising the requirements of Problem 1. However, to take advantage of these insights, a solution of the Hamilton-Jacobi-Bellman PDE (4) or (5) is required. Typically, closed-form solutions of the HJB PDE are not available and numerical approaches to solve the PDE are cursed with high computational demands. Thus, alternative design approaches based on Pontryagin's Minimum principle and the *Hamilton Conditions* (see [21], [6], [7] for insightful discussions on the relation between PMP and DP) are often preferred in applications. The Hamilton conditions are trajectory-based and therefore computed only for specific initial states. Moreover, these requirements provide, in general, only necessary conditions of optimality. This alternative approach is summarised in the remainder of this section.

Let $\mathcal{H} : \mathbb{R}^n \times \mathbb{R}^n \to \mathbb{R}$ denote the (minimised) Hamiltonian function associated with the optimal control problem (1), *i.e.*

$$\mathcal{H}(x, \lambda) = \frac{1}{2}q(x) + \lambda^\top f(x) - \frac{1}{2}\lambda^\top g(x) g(x)^\top \lambda\,, \tag{6}$$

where $\lambda(t) \in \mathbb{R}^n$ is the *costate* variable. Provided that $V^\star(x_0)$ is $C^2(\mathcal{X})$ for a certain $\mathcal{X} \subseteq \mathbb{R}^n$, as implied by the data of the problem for $x_0 \in \mathcal{X}$ (see Remark 1) the optimal process $x^\star$, *i.e* the trajectory of (1b) in closed-loop with the optimal control, evolves according to the dynamics (Hamilton conditions)

$$\begin{bmatrix} \dot{x} \\ \dot{\lambda} \end{bmatrix} = J\nabla\mathcal{H}(x, \lambda) := X_\mathcal{H}(x, \lambda)\,, \tag{7}$$

from the initial condition $(x_0, \nabla V^\star(x_0))$, with

$$J = \begin{bmatrix} 0 & I_n \\ -I_n & 0 \end{bmatrix}. \tag{8}$$

Let $\varphi_\mathcal{H}(t; x_0, \lambda_0)$ denote the *flow* of the Hamiltonian dynamics (7), which is assumed to be complete, at time t and from the initial condition (x_0, λ_0), and let $\pi_x \circ \varphi_\mathcal{H}$ and $\pi_\lambda \circ \varphi_\mathcal{H}$ denote the projections of the flow on the x components and on the λ components, respectively, of the state/costate space. Since the conditions in Assumption 1 imply that the system (1b) is locally exponentially stabilizable and detectable from the (virtual) output $y = q(x)$, it follows, by [24, Section 6] that the Hamiltonian dynamics (7) possesses a *hyperbolic* equilibrium point at $(x, \lambda) = (0, 0)$ with n-dimensional global stable $\mathcal{N}^s$ and unstable $\mathcal{N}^u$ submanifolds through the origin that are invariant for the system (7). The interested reader is referred to [25] for similar results in the

This work is licensed under a Creative Commons Attribution 4.0 License. For more information, see https://creativecommons.org/licenses/by/4.0/

This article has been accepted for publication in IEEE Transactions on Automatic Control. This is the author's version which has not been fully edited and content may change prior to final publication. Citation information: DOI 10.1109/TAC.2022.3230764

case of nonlinear H_∞ control problems in which the arising Hamiltonian dynamics are structurally identical to those in (7). In addition, recalling that the stable and unstable submanifolds of a Hamiltonian system are *Lagrangian* (see *e.g.* [25, Lemma 1]), one has that such submanifolds are locally described as the graph of closed one-forms, namely $\mathcal{N}^s = \text{graph}(\nabla V^s)$ and $\mathcal{N}^u = \text{graph}(\nabla V^u)$, respectively, for some generating functions $V^s : \mathbb{R}^n \to \mathbb{R}$ and $V^u : \mathbb{R}^n \to \mathbb{R}$ that constitute smooth solutions to the HJB equation (4). Finally, note that the stable (unstable, respectively) invariant submanifold is tangent at the origin to the n-dimensional subspace W^s (W^u, respectively) described by the eigenspace of the linearized Hamiltonian system associated with eigenvalues with negative (positive, respectively) real parts of the Hamiltonian matrix

$$H := \begin{bmatrix} A & -BB^\top \\ -Q & -A^\top \end{bmatrix}. \tag{9}$$

As a consequence, the origin of the state-space is a locally asymptotically stable equilibrium point of the (*forward-time*) closed-loop dynamics $\dot{x} = f(x) - g(x)g(x)^\top \nabla V^s$, $x(0) = x_0$ and of the (*backward-time*) dynamics $\dot{x} = -(f(x) - g(x)g(x)^\top \nabla V^u)$, $x(0) = x_0$. Moreover, the optimal costate $\lambda^\star : \mathbb{R} \to \mathbb{R}^n$ in (7) satisfies $\lambda^\star(t) = \nabla V^s(x^\star(t))$, for any $t \geqslant 0$ (and, provided the problem satisfies the aforementioned conditions, under which the DP method provides necessary *and* sufficient conditions of optimality, $V^\star = V^s$).

III. Finite-dimensional characterisation of optimal control laws

To provide a concise statement of the following result - which yields a finite-dimensional, static characterisation of the solution of Problem 1 - consider a vector $\mathbf{s} = [s_1\ s_2\ \dots\ s_{2n-1}]^\top \in \mathbb{R}^{2n-1}$ and a scalar positive constant $\varepsilon \in \mathbb{R}_{>0}$, and define the vector-valued function $\alpha : \mathbb{R}^{2n-1} \to \mathbb{R}^{2n}$ according to

$$\alpha(\mathbf{s}) := \begin{bmatrix} \varepsilon\cos(s_1) \\ \varepsilon\sin(s_1)\cos(s_2) \\ \varepsilon\sin(s_1)\sin(s_2)\cos(s_3) \\ \vdots \\ \varepsilon\sin(s_1)\dots\sin(s_{2n-2})\cos(s_{2n-1}) \\ \varepsilon\sin(s_1)\dots\sin(s_{2n-2})\sin(s_{2n-1}) \end{bmatrix}. \tag{10}$$

The mapping α describes the Cartesian coordinates of points on the hypersphere of radius ε in $\mathbb{R}^{2n}$, namely the set $\mathcal{S}_\varepsilon := \{(x,\lambda) \in \mathbb{R}^n \times \mathbb{R}^n : \|(x,\lambda)\| = \varepsilon\} \subset \mathbb{R}^{2n}$ for the elements s_i ranging in the set $[0,\ 2\pi)$, $i = 1, ..., 2n-1$. Casting the problem in terms of the angular coordinates $\mathbf{s}$, rather than the original (x,λ) coordinates, is central to the construction of a static, *unconstrained* optimisation problem characterising the solution of Problem 1. Nonetheless, the specific selection of the parameterisation in (10) may be replaced by alternative descriptions. In the following it is assumed that, whenever $\mathbf{s}$ consists of a set of (potentially infinitely many) values $\mathbf{s} = \{\mathbf{s}^i\}_{i\in\mathcal{I}\subseteq\mathbb{R}}$, the application of the function $\alpha(\cdot)$ to the set $\mathbf{s}$ denotes in turn the set $\alpha(\mathbf{s}) := \{\alpha(\mathbf{s}^i)\}_{i\in\mathcal{I}}$. Finally, let $\hat{\varphi}(x_0,\lambda_0)$ define the *locus of points* along a specific trajectory of the Hamiltonian dynamics (7), namely $\hat{\varphi}(x_0,\lambda_0) := \{(x,\lambda) \in \mathbb{R}^n \times \mathbb{R}^n : \exists\, \hat{t} \in \mathbb{R} \text{ s.t. } (x,\lambda) = \varphi_{\mathcal{H}}(\hat{t}; x_0, \lambda_0)\}$. Recall that $V^s : \mathbb{R}^n \to \mathbb{R}$ and $V^u : \mathbb{R}^n \to \mathbb{R}$ locally describe the generating functions for the stable and unstable invariant submanifolds of (7), respectively. Consider the function

$$\mathcal{C}_{x_0}(\mathbf{s},\tau_1,\tau_2) := \|\pi_x \circ \varphi_{\mathcal{H}}(-\tau_1; \alpha(\mathbf{s})) - x_0\|^2 + \|\varphi_{\mathcal{H}}(\tau_2; \alpha(\mathbf{s}))\|^2. \tag{11}$$

The first term of (11) quantifies the distance between the initial condition x_0 and the trajectory of the Hamiltonian dynamics (7) starting from the point $\alpha(\mathbf{s})$ and propagated in backward or forward time (for τ_1 positive or negative, respectively). The second term, instead, quantifies the distance between the origin and the trajectory of the Hamiltonian dynamics (7) starting from the point $\alpha(\mathbf{s})$ and propagated in forward or backward time (for τ_2 positive or negative, respectively). The following result shows that the Hamiltonian system (7) has the property that the minimum of $\mathcal{C}_{x_0}$ can be obtained by two trajectories only, namely those associated with its stable and unstable submanifolds and passing through x_0. Moreover, such trajectories can be parameterized by the intersection point $\alpha(\mathbf{s}) \in \mathcal{S}_\varepsilon$, together with the times τ_1 and τ_2. As a consequence, the solution of Problem 1 can be equivalently characterised by the static, unconstrained minimisation of (11) with respect to $(\mathbf{s}, \tau_1, \tau_2)$. The above discussion suggests that the solution of Problem 1 can be constructed in two steps.

First, the minimisers of $\mathcal{C}_{x_0}$ (associated to the generating functions V^s and V^u) are computed (see (13) below). This requires detecting the intersections, described by the point $\alpha(\mathbf{s})$ for some $\mathbf{s}$, of two sets: *(i)* the *loci* of points of the trajectories of (7) that *both* converge to the origin *and* have a projection on the state space that contains x_0; *(ii)* the surface of $\mathcal{S}_\varepsilon$. These intersections are identified via the static minimisation of $\mathcal{C}_{x_0}$.

Second, once the intersection $\alpha(\mathbf{s}^\star)$ corresponding to the stable submanifold $\mathcal{N}^s$ has been obtained, the optimal control law is $u^\star(t) = -g(x(t))^\top \lambda(t)$, with $(x(t),\lambda(t))$ the trajectory of (7) corresponding to the initial condition $x(0) = x_0 = \pi_x \circ \varphi_{\mathcal{H}}(-\tau_1^\star; \alpha(\mathbf{s}^\star))$, $\lambda(0) = \pi_\lambda \circ \varphi_{\mathcal{H}}(-\tau_1^\star; \alpha(\mathbf{s}^\star))$.

By inspecting the latter step (*i.e.* a standard forward propagation of certain initial conditions), it is evident that the former (*i.e.* the characterisation and the static minimisation of $\mathcal{C}_{x_0}$) constitutes the crucial aspect of the construction of the optimal control law. Hence, in what follows attention is focused mainly on this first step. The above (intuitive) discussion is formalised in the following statements.

Theorem 1. *Let $x_0 \in \mathcal{X} \subseteq \mathbb{R}^n$ be given and consider the infinite-horizon optimal control problem $\mathcal{Q}_{x_0}$. Suppose that V^s and V^u are $C^2(\mathcal{X})$. Fix a sufficiently small $\varepsilon > 0$ and suppose that Assumption 1 holds. Then*

$$\alpha(\boldsymbol{s}^\star) = (\hat{\varphi}(x_0, \nabla V^s(x_0)\,) \cap \mathcal{S}_\varepsilon) \cup (\hat{\varphi}(x_0, \nabla V^u(x_0)\,) \cap \mathcal{S}_\varepsilon)\ , \tag{12}$$

where[2] $\boldsymbol{s}^\star \in [0,\ 2\pi)^{2n-1}$, is such that there exists $\tau_1^\star \in \mathbb{R}$ with

[2]The notation $[a,b]^k$ describes the product set $[a,b] \times [a,b] \times \dots \times [a,b]$, repeated k times.

This work is licensed under a Creative Commons Attribution 4.0 License. For more information, see https://creativecommons.org/licenses/by/4.0/

This article has been accepted for publication in IEEE Transactions on Automatic Control. This is the author's version which has not been fully edited and content may change prior to final publication. Citation information: DOI 10.1109/TAC.2022.3230764

the property that

$$\lim_{\tau_2 \to \varpi} \mathcal{C}_{x_0}(\boldsymbol{s}^\star, \tau_1^\star, \tau_2) = 0\,, \tag{13}$$

with ϖ equal to either $-\infty$ or $+\infty$. ∘

Remark 2. Relying on the definition of the extended real line $\bar{\mathbb{R}}$, the intuition behind Theorem 1 can be captured by abusing the notation (*i.e.* letting a *minimizer* belong to $\bar{\mathbb{R}}$): the values $\mathbf{s}^\star$ are those that belong to the set $(\mathbf{s}^\star, \tau_1^\star, \tau_2^\star) := \{(\mathbf{s}, \tau_1, \tau_2) \in \Xi : (\mathbf{s}, \tau_1, \tau_2) \in \arg\min_{(\mathbf{s},\tau_1,\tau_2)\in\Xi} \mathcal{C}_{x_0}(\mathbf{s}, \tau_1, \tau_2)\}$, with $\Xi = [0,\, 2\pi)^{2n-1} \times \bar{\mathbb{R}} \times \bar{\mathbb{R}}$. ▲

Proof: The claim is demonstrated by showing that the inclusions

$$\alpha(\mathbf{s}^\star) \supseteq (\hat{\varphi}(x_0, \nabla V^s(x_0))\,) \cap \mathcal{S}_\varepsilon) \cup (\hat{\varphi}(x_0, \nabla V^u(x_0))\,) \cap \mathcal{S}_\varepsilon) \tag{14}$$

and

$$\alpha(\mathbf{s}^\star) \subseteq (\hat{\varphi}(x_0, \nabla V^s(x_0))\,) \cap \mathcal{S}_\varepsilon) \cup (\hat{\varphi}(x_0, \nabla V^u(x_0))\,) \cap \mathcal{S}_\varepsilon) \tag{15}$$

hold simultaneously.

Consider first the inclusion (14), which is verified provided the cost function $\mathcal{C}_{x_0}$ obtains its infimum value, relatively to $\mathbf{s}$ in Ξ, at the intersection between the trajectory identified by $\hat{\varphi}(x_0, \nabla V^s(x_0))$ (similarly for V^u) and the ball of radius ε. The *initial value problem* defined by the dynamics (7) and a generic initial condition $(x_0, \lambda_0) \in \mathbb{R}^n \times \mathbb{R}^n$ admits a unique solution locally around the origin of the state-costate space, which is continuous with respect to time and such that the limit for t that tends to $+\infty$ ($-\infty$, respectively) is equal to zero for any initial condition in the stable $\mathcal{N}^s$ (unstable $\mathcal{N}^u$, respectively) invariant submanifold of (7). Thus, it follows that the intersection between $\hat{\varphi}(x_0, \nabla V^s(x_0))$ ($\hat{\varphi}(x_0, \nabla V^u(x_0))$, respectively) with $\mathcal{S}_\varepsilon$, for sufficiently small ε, contains a single point $z^s \in \mathbb{R}^{2n}$ ($z^u \in \mathbb{R}^{2n}$, respectively) such that the infimum with respect to τ_2 in $\bar{\mathbb{R}}$ of the second term of $\mathcal{C}_{x_0}$ in (11), *i.e.* the limit (13), can be zero. Moreover, by definition of $\hat{\varphi}(\cdot,\cdot)$, z^s is such that also the first term of $\mathcal{C}_{x_0}$ is zero for some $\tau_1 \in \mathbb{R}$ since $z^s \in \hat{\varphi}(x_0, \nabla V^s(x_0))$. Therefore, since $\mathcal{C}_{x_0}$ is clearly non-negative and since z^s satisfies $\|z^s\| = \varepsilon$ by definition of $\mathcal{S}_\varepsilon$, if follows that $z^s \in \alpha(\mathbf{s}^\star)$. An identical reasoning can be carried out for z^u, hence showing (14).

To prove the converse inclusion (15) note that the function $\varphi_{\mathcal{H}}(\cdot; z_0)$ is continuous in $\bar{\mathbb{R}}$ and $\varphi_{\mathcal{H}}(\pm\infty; z_0) = \lim_{t\to\pm\infty} \varphi_{\mathcal{H}}(t; z_0)$. Thus, it must be shown that there does not exist any point $\tilde{z} \in \mathbb{R}^{2n}$, with norm equal to ε, other than z^s and z^u, at which $\mathcal{C}_{x_0}(\tilde{z}, \tau_1, \tau_2) = 0$ for some $\tau_1 \in \bar{\mathbb{R}}$ and $\tau_2 \in \bar{\mathbb{R}}$. To this end, suppose initially that there exists such a point $\tilde{z}$ that does not belong to $\mathcal{N}^s \cup \mathcal{N}^u$. Then clearly $\inf_{\tau_2\in\bar{\mathbb{R}}} \|\varphi_{\mathcal{H}}(\tau_2; \tilde{z})\|^2$ is strictly greater than zero, since the trajectory ensuing from $\tilde{z}$ does not tend to the origin neither in forward nor in backward time. If instead $\tilde{z} \in \mathcal{N}^s \setminus \hat{\varphi}(x_0, \nabla V^s(x_0))$ (an identical discussion can be carried out for the case of the unstable invariant submanifold $\mathcal{N}^u$), then $\inf_{\tau_1\in\bar{\mathbb{R}}} \|\pi_x \circ \varphi_{\mathcal{H}}(-\tau_1; \tilde{z}) - x_0\|^2$ is strictly greater than zero by definition of the set $\hat{\varphi}(x_0, \nabla V^s(x_0))$ and of the distance between such a set and the locus of points defined by $\varphi_{\mathcal{H}}(t; \tilde{z})$ for any $t \in \bar{\mathbb{R}}$. The proof is concluded by recalling that $\hat{\varphi}(x_0, \nabla V^s(x_0))$ (and similarly for $V^u(x_0)$) contains a single point with norm equal to ε, namely z^s (z^u, equivalently). □

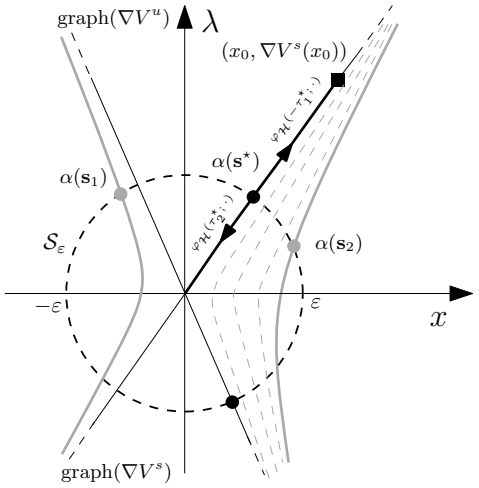

Fig. 1. Graphical illustration of the statement of Theorem 1. The solid black circles constitute the set $\boldsymbol{\alpha(\mathbf{s}^\star)}$. The solid black line depicts the forward/backward flow of the optimal set along the Hamiltonian dynamics, which is such that $\boldsymbol{\mathcal{C}_{x_0}(\mathbf{s}^\star, \tau_1^\star, \tau_2^\star) = 0}$. Any other trajectory of the Hamiltonian dynamics that intersects the set $\boldsymbol{\mathcal{S}_\varepsilon}$ (depicted by the gray lines) is such that either the first or the second term of $\boldsymbol{\mathcal{C}_{x_0}(\cdot, \tau_1, \tau_2)}$ is strictly positive for any $\boldsymbol{\tau_1 \in \bar{\mathbb{R}}}$ and $\boldsymbol{\tau_2 \in \bar{\mathbb{R}}}$.

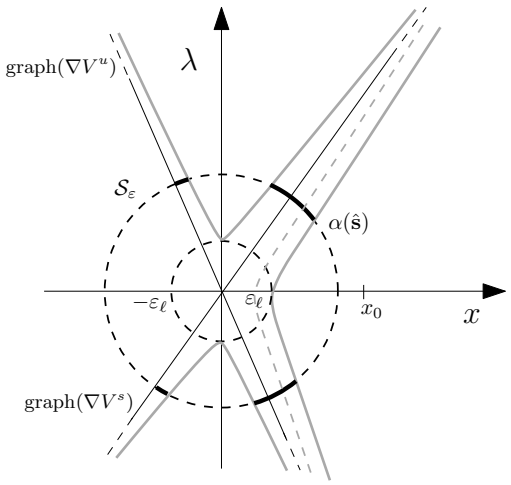

Fig. 2. Graphical illustration of the statement of Theorem 2. The solid segments on the set $\boldsymbol{\mathcal{S}_\varepsilon}$ indicate the arguments which attain the minimum of $\boldsymbol{\mathcal{C}^{\varepsilon_\ell}_{x_0}}$. These constitute intermediate points of all trajectories of the Hamiltonian system (7) that satisfy the initial condition $\boldsymbol{x(0) = x_0}$ *and* that (in finite time) enter (depicted by the gray, dashed line) or are tangent (depicted by the gray, solid lines) to the set $\boldsymbol{\mathcal{S}_{\varepsilon_\ell}}$.

The proposed results seemingly share common ingredients with strategies that aim at a trajectory-based characterisation of certain invariant manifolds for nonlinear systems as well as with the class of the so-called shooting methods, which possess a long history in the literature. Therefore, it is worth stressing the particular features of the method discussed herein, which significantly distinguish them from the two above-mentioned frameworks. First, differently from the former, the objective here is not to approximate the entire manifold but rather a *single* trajectory with certain properties. Differently

This work is licensed under a Creative Commons Attribution 4.0 License. For more information, see https://creativecommons.org/licenses/by/4.0/

This article has been accepted for publication in IEEE Transactions on Automatic Control. This is the author's version which has not been fully edited and content may change prior to final publication. Citation information: DOI 10.1109/TAC.2022.3230764

from the latter, instead of considering only the forward propagation from a prescribed boundary condition, the desired trajectory is computed by determining its intersection with a hypersphere centered at the origin. In fact, the key idea consists in the *simultaneous forward and backward* propagation of trajectories from points lying on the surface of the hypersphere. As a consequence one obtains a computationally amenable method that hinges upon the *unconstrained minimisation* of a certain function (see (11)). Furthermore, since the radius of the hypersphere can be selected arbitrarily small, differently from standard shooting methods over relatively long horizons, the knowledge of the linearized solution becomes a valid initial guess for the nonlinear iterations (see the more detailed discussion in Remark 5 below). Finally, it is worth mentioning that, as a side-effect of relying on a completely unconstrained minimisation (namely without even restricting the sign of the time variables τ_1 and τ_2 in (11)), the minimum of the equivalent cost function is obtained also at a trajectory that belongs to the unstable invariant manifold.

Remark 3. Theorem 1 establishes that the (static) minimisation of the function $\mathcal{C} : \Xi \to \mathbb{R}_{\geqslant 0}$, parameterised with respect to the initial state $x_0 \in \mathbb{R}^n$, characterises the intersection points between the trajectories associated with the solutions $V^s(x_0)$ and $V^u(x_0)$ of the HJB PDE lying on the stable and unstable Lagrangian submanifolds of (7), respectively, with the hypershere of radius ε in the state/costate space. ▲

Remark 4. As noted in the proof of Theorem 1, for a given initial state x_0 there are (only) two initial conditions λ_0, such that the resulting trajectories of the Hamiltonian system (7) converge to the origin in either forward or backward time. The set $\alpha(\mathbf{s}^\star)$ contains the two intersection points between these trajectories and the ball of radius ε. The equation (12) entails that the knowledge of the intersection point corresponding to the trajectory belonging to the stable submanifold, *i.e.* z^s, permits the computation of the optimal initial condition for the costate variable $\lambda_0 = \nabla V^s(x_0)$ by integrating *backward in time* the Hamiltonian dynamics (7). The relation $\varphi_{\mathcal{H}}(-\tau_1^\star, \alpha(\mathbf{s}^\star)) \subseteq \operatorname{graph} \nabla_x V^s \cup \operatorname{graph} \nabla_x V^u$ suggests that by considering a certain number of suitably selected initial conditions $x_{0,i}$ and by determining minimum points of $\mathcal{C}_{x_{0,i}}$ it is possible to envision a strategy to reconstruct the stable and unstable invariant submanifolds, which would in turn yield the gradient of the value function V^s without explicitly solving the HJB PDE (4). The objective of this paper is, however, different: rather than determining the invariant manifolds, the objective is to determine (or approximate) the trajectory of the Hamiltonian system corresponding to the optimal process, and thereby construct the optimal control law, for a *specific* initial condition of (1b). ▲

Remark 5. The intuition of forward propagating the trajectories of the underlying Hamiltonian dynamics to determine the solution to an optimal control problem has been explored in the literature before, especially in the case of finite-horizon problems, see *e.g.* [26] and references therein. Due to the intrinsic instability of the Hamiltonian dynamics, the so-called *shooting methods* necessarily require an accurate initial guess of the costate initial condition $\lambda(0)$ or a (short) bounded time interval even in the case of infinite-horizon problems. A novel feature of the method proposed herein is that the optimal state/costate trajectory is not approximated by considering only the *forward* propagation from certain initial conditions (as is common in the literature), but by characterisating the intersection of such a trajectory with a hypershpere, namely *by forward and backward* propagating the trajectory from an intermediate point that belongs to the surface of the hypersphere. Provided the radius of the hypersphere is selected sufficiently small, the interesection to be determined is (much) closer to the origin than x_0. Thus a valid initial guess for the *intermediate* point on the boundary of the hypersphere may indeed be suggested by the linearized solution, *i.e.* by letting $\mathbf{s}(0) \in \mathbb{R}^{2n-1}$ be such that

$$\alpha(\mathbf{s}(0)) := \varepsilon \begin{bmatrix} x_0 \\ Px_0 \end{bmatrix} \Big/ \left\| \begin{bmatrix} x_0 \\ Px_0 \end{bmatrix} \right\|. \tag{16}$$

Such strategy is employed and illustrated in the numerical simulations of Section V. ▲

Remark 6. The main objective of this paper - namely to provide a finite-dimensional characterisation of the solution in infinite-horizon optimal control problems - is similar in spirit to that of the well-known Model Predictive Control (MPC) strategies, see *e.g.* [27] and references therein. However, a few relevant differences should be highlighted. In MPC the finite-dimensional characterisation is obtained by considering a *time quantisation* over a finite, typically short, time interval around the current value of the state: this allows one to pose a static optimisation task with respect to the (finite) samples of the underlying control law. However, in continuous-time nonlinear system - since portions of trajectories that are optimal over a finite-horizon are not, in general, restrictions of the optimal control law over the entire horizon - such a strategy inevitably introduces a residual approximation error even in the nominal case of perfect knowledge of the plant and absence of noise or disturbances. Theorem 1 instead provides a finite-dimensional *exact* characterisation of the optimal control law over the entire infinite horizon. Therefore, even in a receding-horizon implementation of the constructions proposed here, potentially in the presence of disturbances, the proposed strategy allows one to employ *moving windows* of length significantly larger than alternative receding horizon strategies in general. This feature is illustrated via a comparative study in Section V. ▲

The intuition behind Theorem 1 is illustrated for the *scalar* case, namely with $n = 1$, in Figure 1, where the black circles constitute the set $\alpha(\mathbf{s}^\star)$, namely the intersections of $\hat{\varphi}(x_0, \nabla V^s(x_0))$ and $\hat{\varphi}(x_0, \nabla V^u(x_0))$, which in the scalar case coincide with $\mathcal{N}^s$ and $\mathcal{N}^u$, respectively, with the set $\mathcal{S}_\varepsilon$. The solid black line represents the forward/backward flow of the optimal set along the Hamiltonian dynamics, which is such that $\mathcal{C}_{x_0}(\mathbf{s}^\star, \tau_1^\star, \tau_2^\star) = 0$. As shown in the proof of Theorem 1, any other trajectory of the Hamiltonian dynamics that intersects the set $\mathcal{S}_\varepsilon$ (represented by the gray lines) is such that either the first (for $\alpha(\mathbf{s}_1)$) or the second (for $\alpha(\mathbf{s}_2)$) term of $\mathcal{C}_{x_0}(\cdot, \tau_1, \tau_2)$ is strictly positive for any $\tau_1 \in \bar{\mathbb{R}}$ and $\tau_2 \in \bar{\mathbb{R}}$.

Remark 7. The discussion in the proof of Theorem 1 suggests two further implications on the values $\tau_1^\star$ and $\tau_2^\star$. First, it is

This work is licensed under a Creative Commons Attribution 4.0 License. For more information, see https://creativecommons.org/licenses/by/4.0/

This article has been accepted for publication in IEEE Transactions on Automatic Control. This is the author's version which has not been fully edited and content may change prior to final publication. Citation information: DOI 10.1109/TAC.2022.3230764

evident that the infimum of $\mathcal{C}_{x_0}$ is obtained by considering the limit of $\tau_2^\star \in \bar{\mathbb{R}}$ to $\pm\infty$, as implied by (13). Moreover, one has that $\tau_1^\star \tau_2^\star > 0$, *i.e.* the infimum is obtained by *simultaneous* forward/backward evaluation of Hamiltonian trajectories. ▲

Remark 7 motivates the result below, which allows one to approximate the solution of $\mathcal{Q}_{x_0}$ with an arbitrary degree of accuracy. Let $\mathcal{V}$ and $\mathcal{W}$ be two non-empty sets and define the *Hausdorff distance* between $\mathcal{V}$ and $\mathcal{W}$, denoted $\mathrm{d}_H(\mathcal{V},\mathcal{W})$, as

$$\mathrm{d}_H(\mathcal{V},\mathcal{W}) = \max\left\{\sup_{v\in\mathcal{V}}\inf_{w\in\mathcal{W}}\|v-w\|, \sup_{w\in\mathcal{W}}\inf_{v\in\mathcal{V}}\|v-w\|\right\}, \tag{17}$$

i.e. defining the largest among all the distances between the points in one set and the closest point in the other set.

Theorem 2. *Let $x_0 \in \mathcal{X} \subseteq \mathbb{R}^n$ be given and consider the infinite-horizon optimal control problem $\mathcal{Q}_{x_0}$. Suppose that V^s and V^u are $C^2(\mathcal{X})$. Fix $\varepsilon > 0$ sufficiently small, and suppose that Assumption 1 holds. Define*

$$\begin{aligned}\mathcal{C}_{x_0}^{\varepsilon_\ell}(\boldsymbol{s},\tau_1,\tau_2) :=& \|\pi_x \circ \varphi_{\mathcal{H}}(-\tau_1;\alpha(\boldsymbol{s})) - x_0\|^2 \\ &+ \max\{0, \|\varphi_{\mathcal{H}}(\tau_2;\alpha(\boldsymbol{s}))\|^2 - \varepsilon_\ell^2\}\,,\end{aligned} \tag{18}$$

where $\varepsilon_\ell \in \mathbb{R}_{>0}$ and $\varepsilon_\ell < \varepsilon$. Then for any $\mu > 0$ there exist $\theta_1, \theta_2, \varepsilon_\ell \in \mathbb{R}_{>0}$ such that

$$\mathrm{d}_H(\alpha(\boldsymbol{s}^\star), \alpha(\hat{\boldsymbol{s}})) < \mu \tag{19}$$

where[3] $(\hat{\boldsymbol{s}},\hat{\tau}_1,\hat{\tau}_2) := \arg\min_{(\boldsymbol{s},\tau_1,\tau_2)\in\Theta} \mathcal{C}_{x_0}^{\varepsilon_\ell}(\boldsymbol{s},\tau_1,\tau_2)$ *and* $\Theta := \{(\boldsymbol{s},\tau_1,\tau_2) \in \Xi : |\tau_1| \leqslant \theta_1, |\tau_2| \leqslant \theta_2\}$. ∘

Proof: First, note that, by continuity of the function $\mathcal{C}_{x_0}^{\varepsilon_\ell}(\mathbf{s},\tau_1,\tau_2)$ with respect to ε_ℓ, $\lim_{\varepsilon_\ell\to 0^+} \mathcal{C}_{x_0}^{\varepsilon_\ell}(\mathbf{s},\tau_1,\tau_2) = \mathcal{C}_{x_0}(\mathbf{s},\tau_1,\tau_2)$, point-wise for any $(\mathbf{s},\tau_1,\tau_2)$, where the latter function is precisely the one defined in (11). Then, let $\mathcal{C}_{x_0,\theta} : \Theta \to \mathbb{R}_{>0}$ be the restriction of the function $\mathcal{C}_{x_0}$ in (11) to the set Θ. Given $\mu > 0$, select $\theta > 0$ and $\mu^\theta < \mu$ such that, letting $\theta_1 = \theta_2 = \theta$ in the definition of Θ,

$$\mathrm{d}_H(\alpha(\mathbf{s}^\star), \alpha(\mathbf{s}^\theta)) < \mu^\theta < \mu\,, \tag{20}$$

where $(\mathbf{s}^\theta, \tau_1^\theta, \tau_2^\theta) := \arg\min_{(\mathbf{s},\tau_1,\tau_2)\in\Theta} \mathcal{C}_{x_0,\theta}(\mathbf{s},\tau_1,\tau_2)$, which exist by continuity of the function $\mathcal{C}_{x_0}$ with respect to its arguments. Therefore, consider a sub-sequence of indices $\{\varepsilon_{\ell,i}\}_{i\in\mathbb{N}}$ such that $\lim_{i\to\infty}\varepsilon_{\ell,i} = 0^+$ and define the corresponding sequence of the functions $\{\mathcal{C}_{x_0}^{\varepsilon_{\ell,i}}\}_{i\in\mathbb{N}}$ with the underlying arguments restricted to the compact domain Θ. By the discussion above, the sequence $\{\mathcal{C}_{x_0}^{\varepsilon_{\ell,i}}\}_{i\in\mathbb{N}}$ converges point-wise to $\mathcal{C}_{x_0,\theta}$ in Θ and each function $\mathcal{C}_{x_0}^{\varepsilon_{\ell,i}}$ is equi-continuous, being a continuous function. Hence, [28, Theorem 7.10] implies also *epi-convergence*[4] of $\{\mathcal{C}_{x_0}^{\varepsilon_{\ell,i}}\}_{i\in\mathbb{N}}$ to $\mathcal{C}_{x_0,\theta}$. Furthermore one has that the restrictions of $\{\mathcal{C}_{x_0}^{\varepsilon_{\ell,i}}\}_{i\in\mathbb{N}}$ to Θ are level-bounded, following from compactness of the corresponding supports, proper and lower semi-continuous for any $i \in \mathbb{N}$. Therefore, by relying on [28, Theorem 7.33] it follows that

$$\limsup_i(\arg\min \mathcal{C}_{x_0}^{\varepsilon_{\ell,i}}) \subset \arg\min \mathcal{C}_{x_0,\theta}\,, \tag{21}$$

and the claim is shown by definition of Hausdorff distance and by the inequality (20). □

Remark 8. Similarly to the interpretation in Remark 3 following the statement of Theorem 1, the rationale behind the formal claim of Theorem 2 can be further explained as follows. The arguments that attain the minimum of function $\mathcal{C}_{x_0}^{\varepsilon_\ell}$ characterise (via the intersection points represented in spherical coordinates $\hat{\mathbf{s}}$) the set of all the trajectories of the Hamiltonian dynamics (7) that enter (in finite time) or are tangent to the set $\mathcal{S}_{\varepsilon_\ell} := \{(x,\lambda) \in \mathbb{R}^n \times \mathbb{R}^n : \|(x,\lambda)\| = \varepsilon_\ell\}$ and whose projection on the state component intersects x_0. The fundamental difference with respect to the characterization of the trajectories as in the statement of Theorem 1 lies in the fact that the minimum of $\mathcal{C}_{x_0}^{\varepsilon_\ell}$ is achieved also at some $|\hat{\tau}_i| < \infty$, namely for certain $(\hat{\mathbf{s}},\hat{\tau}_1,\hat{\tau}_2)$ belonging to the compact set Θ. These observations are illustrated for the scalar case in Figure 2. ▲

IV. Algorithms for minimizing the Hamiltonian trajectory-based cost

The main objective of this section lies in presenting an algorithm that achieves the minimisation of the trajectory-based (finite-dimensional) cost functions defined in (11) and especially (18). After providing a general statement, outlining the design of such algorithm, the discussion is focused on showing how to circumvent specific implementation issues arising by employing standard minimisation techniques. In the following statement we introduce a continuous-time dynamical system, whose (asymptotically stable) equilibrium corresponds to a minimiser of the static cost function (18). This dynamical system constitutes a central component of the algorithm presented in the following subsections. To provide a concise statement of the result, consider the partial derivatives of the function (18) with respect to its arguments, provided in (22) overleaf, and let $\mathbb{B}$ denote a ball of radius one.

Proposition 1. *Let $x_0 \in \mathcal{X} \subseteq \mathbb{R}^n$ be given. Fix $\varepsilon > 0$ and $\varepsilon_\ell > 0$ sufficiently small and any θ_1, $\theta_2 \in \mathbb{R}_{>0}$. Suppose in addition that Assumption 1 holds. Let $\gamma > 0$ and consider*

$$\dot{\eta} = -\gamma \nabla_\eta \mathcal{C}_{x_0}^{\varepsilon_\ell}(\eta)(\nabla_\eta \mathcal{C}_{x_0}^{\varepsilon_\ell}(\eta)^\top \nabla_\eta \mathcal{C}_{x_0}^{\varepsilon_\ell}(\eta))^{-1} \mathcal{C}_{x_0}^{\varepsilon_\ell}(\eta)\,, \tag{23}$$

where $\eta = [\xi,\, \sigma_1,\, \sigma_2] \in \mathbb{R}^{2n+1}$ and $\nabla_\eta \mathcal{C}_{x_0}^{\varepsilon_\ell} = [\nabla_\xi \mathcal{C}_{x_0}^{\varepsilon_\ell}{}^\top, \nabla_{\sigma_1}\mathcal{C}_{x_0}^{\varepsilon_\ell}, \nabla_{\sigma_2}\mathcal{C}_{x_0}^{\varepsilon_\ell}]^\top$. Then, there exist $\mu, c_1, c_2 \in \mathbb{R}_{>0}$ such that

$$\mathrm{d}_H(\alpha(\xi(t)), \alpha(\hat{\boldsymbol{s}})) \leqslant c_1 e^{-c_2\, t} \mathrm{d}_H(\alpha(\xi(0)), \alpha(\hat{\boldsymbol{s}})) \tag{24}$$

for $t \geqslant 0$ and $\eta(0) \in \arg\min_{(\boldsymbol{s},\tau_1,\tau_2)\in\Theta} \mathcal{C}_{x_0}^{\varepsilon_\ell}(\boldsymbol{s},\tau_1,\tau_2) + \mu\mathbb{B}$. ∘

Proof: First, note that the function $\mathcal{C}_{x_0}^{\varepsilon_\ell}$ restricted to Θ is lower semi-continuous, since it is, in fact, continuous, proper and level-bounded. It follows by [28, Theorem 1.9] that the set $(\hat{\mathbf{s}},\hat{\tau}_1,\hat{\tau}_2) := \arg\min_{(\mathbf{s},\tau_1,\tau_2)\in\Theta} \mathcal{C}_{x_0}^{\varepsilon_\ell}$ is non-empty and compact, hence the set $\alpha(\hat{\mathbf{s}})$ is compact. Moreover, by definition of the set $(\hat{\mathbf{s}},\hat{\tau}_1,\hat{\tau}_2)$ (namely, the points in Θ at which $\mathcal{C}_{x_0}^{\varepsilon_\ell}(\mathbf{s},\tau_1,\tau_2) = 0$) and of (local) minimum, it follows that there exists a strictly positive constant $\mu_1 \in \mathbb{R}_{>0}$ such that $\nabla_\eta \mathcal{C}_{x_0}^{\varepsilon_\ell}(\eta)$ is different from zero for any $\eta \in (\hat{\mathbf{s}},\hat{\tau}_1,\hat{\tau}_2) + \mu_1\mathbb{B}$. As a consequence, the (right) pseudo-inverse of the row vector $\nabla_\eta \mathcal{C}_{x_0}^{\varepsilon_\ell}(\eta)^\top \in \mathbb{R}^{2n+1}$, namely $\nabla_\eta \mathcal{C}_{x_0}^{\varepsilon_\ell}(\eta)^\dagger =$

[3] Considerations similar to those discussed in Remark 2 are employed here to characterise the set $(\hat{\mathbf{s}},\hat{\tau}_1,\hat{\tau}_2)$.

[4] The interested reader is referred to [28, Chapter 7] for further definitions and discussions.

This work is licensed under a Creative Commons Attribution 4.0 License. For more information, see https://creativecommons.org/licenses/by/4.0/

This article has been accepted for publication in IEEE Transactions on Automatic Control. This is the author's version which has not been fully edited and content may change prior to final publication. Citation information: DOI 10.1109/TAC.2022.3230764

$$\nabla_{\mathbf{s}}\mathcal{C}^{\varepsilon_\ell}_{x_0} = \begin{cases} 2(\pi_x \circ \nabla_\alpha \varphi_{\mathcal{H}}(-\tau_1;\alpha(\mathbf{s}))\nabla_{\mathbf{s}}\alpha(\mathbf{s}))^\top(\pi_x \circ \varphi_{\mathcal{H}}(-\tau_1;\alpha(\mathbf{s})) - x_0) \\ \quad +2(\nabla_\alpha \varphi_{\mathcal{H}}(\tau_2;\alpha(\mathbf{s}))\nabla_{\mathbf{s}}\alpha(\mathbf{s}))^\top \varphi_{\mathcal{H}}(\tau_2;\alpha(\mathbf{s}))\,, & \text{if } \|\varphi_{\mathcal{H}}(\tau_2;\alpha(\mathbf{s}))\|^2 > \varepsilon_\ell^2 \\ 2(\pi_x \circ \nabla_\alpha \varphi_{\mathcal{H}}(-\tau_1;\alpha(\mathbf{s}))\nabla_{\mathbf{s}}\alpha(\mathbf{s}))^\top(\pi_x \circ \varphi_{\mathcal{H}}(-\tau_1;\alpha(\mathbf{s})) - x_0)\,, & \text{if } \|\varphi_{\mathcal{H}}(\tau_2;\alpha(\mathbf{s}))\|^2 \leqslant \varepsilon_\ell^2 \end{cases} \tag{22a}$$

$$\nabla_{\tau_1}\mathcal{C}^{\varepsilon_\ell}_{x_0} = -2(\pi_x \circ X_{\mathcal{H}}(\alpha(\mathbf{s})))^\top(\pi_x \circ \varphi_{\mathcal{H}}(-\tau_1;\alpha(\mathbf{s})) - x_0) \tag{22b}$$

$$\nabla_{\tau_2}\mathcal{C}^{\varepsilon_\ell}_{x_0} = \begin{cases} 2(\pi_x \circ X_{\mathcal{H}}(\alpha(\mathbf{s})))^\top \varphi_{\mathcal{H}}(\tau_2;\alpha(\mathbf{s}))\,, & \text{if } \|\varphi_{\mathcal{H}}(\tau_2,\alpha(\mathbf{s}))\|^2 > \varepsilon_\ell^2 \\ 0\,, & \text{if } \|\varphi_{\mathcal{H}}(\tau_2;\alpha(\mathbf{s}))\|^2 \leqslant \varepsilon_\ell^2 \end{cases} \tag{22c}$$

$\nabla_\eta \mathcal{C}^{\varepsilon_\ell}_{x_0}(\eta)(\nabla_\eta \mathcal{C}^{\varepsilon_\ell}_{x_0}(\eta)^\top \nabla_\eta \mathcal{C}^{\varepsilon_\ell}_{x_0}(\eta))^{-1}$, is well-defined in the same neighborhood. The remainder of the proof then follows directly from the result of Theorem 2 and standard Lyapunov stability arguments. To this end, note first that the function $C^{\varepsilon_\ell}_{x_0}$ is (locally) positive-definite with respect to the set $(\hat{\mathbf{s}}, \hat{\tau}_1, \hat{\tau}_2)$ and for any $\eta \in (\hat{\mathbf{s}}, \hat{\tau}_1, \hat{\tau}_2) + \mu_2\mathbb{B}$, for some $\mu_2 \in \mathbb{R}_{>0}$, hence it can be employed as a candidate for a Lyapunov function. Moreover, (locally) the dynamics (23) are such that $\dot{C}^{\varepsilon_\ell}_{x_0}(\eta) = -\gamma C^{\varepsilon_\ell}_{x_0}(\eta)$, hence $C^{\varepsilon_\ell}_{x_0}(\eta(t)) = e^{-\gamma t} C^{\varepsilon_\ell}_{x_0}(\eta(0))$ for $t \geqslant 0$. The latter implies that with $\mu := \min\{\mu_1, \mu_2\}$, by continuity of $\alpha(\cdot)$, $\xi(t)$ converges exponentially to $\hat{\mathbf{s}}$. □

Remark 9. The intuition behind the statement of Proposition 1 suggests that each connected component of the set $\alpha(\hat{\mathbf{s}})$ is locally exponentially stable for the dynamics (23). It is worth observing that, for a fixed value of the parameter $\varepsilon_\ell > 0$, while clearly $\alpha(\mathbf{s}^\star) \subset \alpha(\hat{\mathbf{s}})$, there may be instead connected components of $\alpha(\hat{\mathbf{s}})$ that possess empty intersection with $\alpha(\mathbf{s}^\star)$ (see Figure 2 compared with the exact case depicted in Figure 1 for a graphical intuition in the case of scalar systems). Furthermore, note that, by combining the claims of Proposition 1 with those of Theorem 2, one has that the trajectories of system (23) recover in practice the actual solution $\mathbf{s}^\star$ provided ε_ℓ is selected arbitrarily small and θ_i arbitrarily large. ▲

Remark 10. The result of Proposition 1 entails that a *single* static minimisation allows one to compute an essentially open-loop approximation of the entire optimal control policy. Note that the strategy ensures that the resulting trajectory enters the hypersphere $\mathcal{S}_{\varepsilon_\ell}$ in finite time. Within the hypersphere one could, for instance, implement the solution of the linearised problem, which will induce a residual error of the order of $O(\varepsilon_\ell^2)$ on the feedback policy and of the order of $O(\varepsilon_\ell^3)$ on the cost of the optimal solution, namely on the value function. Thus, the resulting strategy (for the *entire* time horizon) can be made arbitrarily accurate through the selection of ε_ℓ. Towards the end of this section we also provide an algorithm (Algorithm 1), in which the static minimisation problem is solved iteratively, yielding a receding-horizon architecture. The receding-horizon architecture has the additional benefit that it can be implemented *on-line* and yields an overall strategy with favourable robustness properties. ▲

By inspecting the equations (22), the dynamics (23) cannot be easily implemented since the underlying vector field depends on the knowledge of the *flow* $\varphi_{\mathcal{H}}(t;\cdot)$ and the *sensitivity*, namely the Jacobian matrix of the flow with respect to the initial condition, whose closed-form expressions are typically not available for nonlinear Hamiltonian dynamics (7). This computational issue can be circumvented via a hybrid implementation. In the following statement standard notation is used to represent the hybrid time domain: $(t;k)$, with $t \in \mathbb{R}_{\geq 0}$ and $k \in \mathbb{N}$, is used to denote the continuous time parameter t along with the index k representing the discontinuous jumps (for reasons of space the interested reader is referred to *e.g* [29] for further details on hybrid systems).

Proposition 2. *Suppose that the assumptions of Proposition 1 hold and consider a hybrid system with state* $\zeta := (\eta, \chi_b, \chi_f, \Psi_b, \Psi_f, \tau) \in \mathbb{R}^{2n+1} \times \mathbb{R}^{2n} \times \mathbb{R}^{2n} \times \mathbb{R}^{2n\times 2n} \times \mathbb{R}^{2n\times 2n} \times \mathbb{R}$, flow dynamics

$$\dot{\eta} = 0\,, \tag{25a}$$
$$\dot{\chi}_b = -(\sigma_1/\tau_M) X_{\mathcal{H}}(\chi_b)\,, \tag{25b}$$
$$\dot{\chi}_f = (\sigma_2/\tau_M) X_{\mathcal{H}}(\chi_f)\,, \tag{25c}$$
$$\dot{\Psi}_b = -(\sigma_1/\tau_M)\nabla X_{\mathcal{H}}(\chi_b)\Psi_b\,, \tag{25d}$$
$$\dot{\Psi}_f = (\sigma_2/\tau_M)\nabla X_{\mathcal{H}}(\chi_f)\Psi_f\,, \tag{25e}$$
$$\dot{\tau} = 1\,, \tag{25f}$$

jump dynamics

$$\eta^+ = \eta + \tau_M F_\gamma(\zeta)\,, \tag{26a}$$
$$\chi_b^+ = \alpha(\xi)\,, \tag{26b}$$
$$\chi_f^+ = \alpha(\xi)\,, \tag{26c}$$
$$\Psi_b^+ = I\,, \tag{26d}$$
$$\Psi_f^+ = I\,, \tag{26e}$$
$$\tau^+ = 0\,, \tag{26f}$$

flow set $C := \{(\eta, \chi, \Psi, \tau) : \tau \leqslant \tau_M\}$ *and* jump set $D := \{(\eta, \chi, \Psi, \tau) : \tau \geqslant \tau_M\}$, *where* $\chi = (\chi_b, \chi_f)$, $\Psi = (\Psi_b, \Psi_f)$,

$$F_\gamma(\zeta) = -\gamma G(\zeta)(G(\zeta)^\top G(\zeta))^{-1}\mathfrak{h}(\eta, \chi, \Psi), \tag{27}$$

with

$$\mathfrak{h}(\eta, \chi, \Psi) := \|\pi_x \circ \chi_b - x_0\|^2 + \max\{0, \|\chi_f\|^2 - \varepsilon_\ell^2\}\,, \tag{28}$$

and $G(\zeta) := [G_1(\zeta)^\top, G_2(\zeta), G_3(\zeta)]^\top$ *as specified in* (29) *overleaf. Then there exists* $\tau_M^\star > 0$ *with the property that the*

This work is licensed under a Creative Commons Attribution 4.0 License. For more information, see https://creativecommons.org/licenses/by/4.0/

This article has been accepted for publication in IEEE Transactions on Automatic Control. This is the author's version which has not been fully edited and content may change prior to final publication. Citation information: DOI 10.1109/TAC.2022.3230764

trajectories of (25), (26) *are such that* $\lim_{t+k\to\infty}\alpha(\xi(t,k))\in\alpha(\hat{\boldsymbol{s}})$ *for any* $\tau_M\in(0,\tau_M^\star)$. ∘

Proof: To begin with, let t_i denote the continuous time at which the i-th jump occurs. Note that the flow dynamics (25f) is such that τ increases at the same rate as the underlying continuous-time component of the hybrid time domain until it reaches $\tau\geq\tau_M$, at which point a jump occurs and its value is "reset" to zero, namely it behaves as a *timer* variable. Thus, regardless of the initial condition of the state of the hybrid system, the hybrid arcs exhibit non-empty continuous time interval with the property that $t_{k+1}-t_k=\tau_M$, for any $k>0$, followed by (periodic) jumps. Note also that η remains constant during flows. Dynamics (25b) and (26b) are such that

$$\chi_b(t_k+\rho,k)=\chi_b(t_k,k)+\int_{t_k}^{t_k+\rho}(-\sigma_1/\tau_M)X_{\mathcal{H}}(\chi_b)\mathrm{d}t\,,$$

for any $\rho\leq\tau_M$ and any $k>0$. Moreover,

$$\begin{aligned}&\chi_b(t_k+\tau_M,k)=\chi_b(t_{k+1},k)=\alpha(\xi(t_k,k))\\&+\int_{-\sigma_1(t_k,k)}^{0}X_{\mathcal{H}}(\chi_b)\mathrm{d}t=\varphi_{\mathcal{H}}(-\sigma_1(t_k,k),\alpha(\xi(t_k,k)))\,.\end{aligned}\tag{30}$$

Similarly, (25c) and (26c) are such that $\chi_f(t_{k+1},k)=\varphi_{\mathcal{H}}(\sigma_2(t_k,k),\alpha(\xi(t_k,k)))$, for any $k>0$. Furthermore, by comparing the structure of (22) and of (29), it is clear that the rationale behind the dynamics (25d) and (25e) consists precisely in yielding the Jacobian matrix of the (unknown) flow of the Hamitonian dynamics (7) with respect to the initial condition. To show this claim, let $\Psi:\mathbb{R}\to\mathbb{R}^{2n\times 2n}$ denote the *sensitivity* of the flow $\varphi_{\mathcal{H}}(t,z_0)$ with respect to z_0, namely $\Psi(t)=\nabla_{z_0}\varphi_{\mathcal{H}}(t,z_0)$, where $z_0\in\mathbb{R}^{2n}$ denotes the initial condition of the flow. Recalling that, by definition, the flow satisfies the fixed-point condition

$$\varphi_{\mathcal{H}}(t,z_0)=z_0+\int_0^t X_{\mathcal{H}}(\varphi_{\mathcal{H}}(s,z_0))\mathrm{d}s\,,\tag{31}$$

it follows that the sensitivity satisfies the relation

$$\nabla_{z_0}\varphi_{\mathcal{H}}(t,z_0)=:\Psi(t)=I+\int_0^t\nabla X_{\mathcal{H}}(z(s))\Psi(s)\mathrm{d}s\,.\tag{32}$$

Thus, it follows from (30) (noting also that σ_1 and σ_2 are constant during flows, namely for any $t\in(t_k,t_{k+1}]$) that the dynamics (25d) and (26d) are such that

$$\begin{aligned}\Psi_b(t_{k+1},k)&=I+\int_{-\sigma_1}^{0}\nabla X_{\mathcal{H}}(\chi_b(s,k))\Psi_b(s,k)\mathrm{d}s\\&=I+\int_{-\sigma_1}^{0}\nabla X_{\mathcal{H}}(\varphi_{\mathcal{H}}(-\sigma_1(t_k,k),\alpha(\xi(t_k,k)))\Psi_b(s,k)\mathrm{d}s\\&=I+\int_{-\sigma_1}^{0}\nabla_\alpha X_{\mathcal{H}}(\varphi_{\mathcal{H}}(-\sigma_1(t_k,k),\alpha(\xi(t_k,k)))\Psi_b(s,k)\mathrm{d}s\,,\end{aligned}$$

which is precisely the sensitivity (as given in (32)) of the flow $\varphi_{\mathcal{H}}(-\sigma_1,\alpha(\eta))$. Similarly, it can be shown that

$$\Psi_f(t_{k+1},k)=I+\int_0^{\sigma_2}\nabla_\alpha X_{\mathcal{H}}(\varphi_{\mathcal{H}}(-\sigma_1,\alpha(\xi(t_k,k)))\Psi_f\mathrm{d}s\,,$$

which is the sensitivity of the flow $\varphi_{\mathcal{H}}(\sigma_2,\alpha(\eta))$. As a consequence of the preceding discussion, one has that $\mathfrak{h}(\eta,\chi,\Psi)\big|_{(t_k,k)}=\mathcal{C}^{\ell}_{x_0}(\eta)$ (with $\mathcal{C}^{\ell}_{x_0}$ as defined in (18)) and $G(\eta,\chi,\Psi)\big|_{(t_k,k)}=\nabla\mathcal{C}^{\varepsilon_\ell}_{x_0}(\eta)$ (as defined in (22)). That is, the dynamics (25) and (26) are such that

$$\eta^+=\eta-\tau_M\gamma\nabla_\eta\mathcal{C}^{\varepsilon_\ell}_{x_0}(\eta)(\nabla_\eta\mathcal{C}^{\varepsilon_\ell}_{x_0}(\eta)^\top\nabla_\eta\mathcal{C}^{\varepsilon_\ell}_{x_0}(\eta))^{-1}\mathcal{C}^{\varepsilon_\ell}_{x_0}(\eta)\,.\tag{33}$$

Namely, the sequence $\eta(t_{k+1},k+1)$, for $k\in\mathbb{Z}_{>0}$, realizes the discretization, via Euler's method, of the continuous dynamics (23). Recalling the main result of Proposition 1, namely that the set $\alpha(\hat{\mathfrak{s}})$ is locally exponentially stable for the continuous dynamics (23), it follows that for sufficiently small τ_M, the set $\alpha(\hat{\mathfrak{s}})$ is locally exponentially stable for the discretized dynamics (33). □

Remark 11. The intuition behind the formal statement of Proposition 2 can be summarized as follows. The state τ of the hybrid system (25)-(26) essentially represents a "sampling time" and the system is such that at jumps χ and Ψ are "initialised" in a manner that ensures that, via the flow dynamics, χ_b and χ_f determine the backwards and forward flows of the Hamiltonian system, whereas Ψ_b and Ψ_f determine the sensitivities of the backwards and forwards flows, respectively. Namely, it is possible to periodically determine the flows and their sensitivities, for which analytical expressions are, in general, not available, required to integrate the continuous dynamics (23) of Proposition 1. At jumps, this knowledge is then used to implement a discretized version of (23).

The previous discussions and formal statements are finally summarised in the following algorithm, which essentially outlines a *receding-horizon* implementation of the results of Propositions 1 and 2, in which the hyperspheres defined by ε and ε_ℓ are allowed to *shrink*.

Algorithm 1.

(0) **Initialization.** Fix τ_M, τ_{rh}, ν, c_1, c_2, τ_{10}, τ_{20}, γ positive constants, such that $c_2<c_1$. Let $x_c=x(0)$, $\kappa=1$ and $\tau_{\kappa-1}=\tau_0=0$.

(1) Let $\varepsilon=c_1\|x_c\|$, $\varepsilon_\ell=c_2\|x_c\|$.

(2) Let $\eta(0)=[\xi_c,\tau_{10},\tau_{20}]$ in (25), (26), with ξ_c such that $\alpha(\xi_c)=\varepsilon[x_c^\top,x_c^\top P]^\top/\|[x_c^\top,x_c^\top P]^\top\|$ as in (16) with P denoting the positive definite solution of the ARE (2).

(3) Integrate the hybrid system (25), (26) in $[0,\nu\tau_M]$ and let $\bar\sigma_i=\sigma_i(\nu\tau_M,\nu)$, $\tau_\kappa=\tau_{\kappa-1}+\min\{\tau_{rh},\bar\sigma_1+\bar\sigma_2\}$ and

$$(x_a(t_a),\lambda_a(t_a))=\begin{cases}\chi_b\left(\nu\tau_M-t_a\frac{\tau_M}{\bar\sigma_1},\nu-1\right),\\ \text{for }\ t_a\in[0,\bar\sigma_1]\\ \chi_f\left((\nu-1)\tau_M+\frac{(t_a-\bar\sigma_1)\tau_M}{\delta\tau-\bar\sigma_1},\nu-1\right),\\ \text{for }\ t_a\in[\bar\sigma_1,\delta\tau]\end{cases}\tag{34}$$

with $\delta\tau=\tau_\kappa-\tau_{\kappa-1}$. Define the control law

$$u^\circ(t):=-g(x_a(t-\tau_{\kappa-1}))^\top\lambda_a(t-\tau_{\kappa-1})\,,\tag{35}$$

for $t\in[\tau_{\kappa-1},\tau_\kappa]$.

This work is licensed under a Creative Commons Attribution 4.0 License. For more information, see https://creativecommons.org/licenses/by/4.0/

This article has been accepted for publication in IEEE Transactions on Automatic Control. This is the author's version which has not been fully edited and content may change prior to final publication. Citation information: DOI 10.1109/TAC.2022.3230764

$$G_1 = \begin{cases} 2(\pi_x \circ \Psi_b \nabla\alpha(\xi))^\top(\pi_x \circ \chi_b - x_0) + 2(\Psi_f \nabla\alpha(\xi))^\top \chi_f\,, & \text{if } \|\chi_f\|^2 > \varepsilon_\ell^2 \\ 2(\pi_x \circ \Psi_b \nabla\alpha(\xi))^\top(\pi_x \circ \chi_b - x_0)\,, & \text{if } \|\chi_f\|^2 \leqslant \varepsilon_\ell^2 \end{cases} \tag{29a}$$

$$G_2 = -2(\pi_x \circ X_{\mathcal{H}}(\alpha(\xi))^\top(\pi_x \circ \chi_b - x_0) \tag{29b}$$

$$G_3 = \begin{cases} 2(\pi_x \circ X_{\mathcal{H}}(\alpha(\xi)))^\top \chi_f\,, & \text{if } \|\chi_f\|^2 > \varepsilon_\ell^2 \\ 0\,, & \text{if } \|\chi_f\|^2 \leqslant \varepsilon_\ell^2 \end{cases} \tag{29c}$$

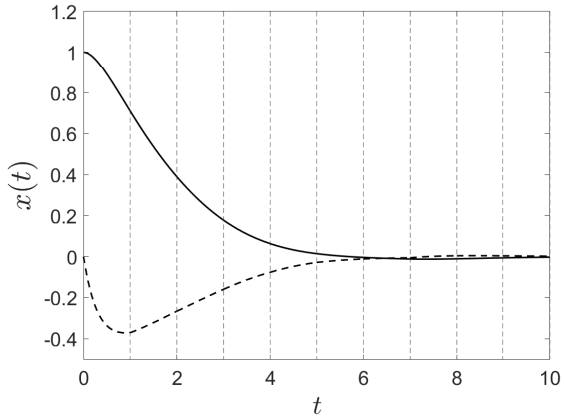

Fig. 3. Time histories of the state $\boldsymbol{x_1(t)}$ (solid line) and $\boldsymbol{x_2(t)}$ (dashed line) of system (37) with $\boldsymbol{x(0) = (1, 0)}$, in closed-loop with the control law determined by Algorithm 1, with $\boldsymbol{\tau_M = 0.01s}$, $\boldsymbol{\tau_{rh} = 1s}$, $\boldsymbol{\nu = 6 \cdot 10^5}$, $\boldsymbol{c_1 = 0.5}$, $\boldsymbol{c_2 = 0.1}$, $\boldsymbol{\tau_{10} = \tau_{20} = 1}$ and $\boldsymbol{\gamma = 0.1}$. The dashed vertical lines represent the time instants $\boldsymbol{\tau_\kappa}$ defined in Algorithm 1.

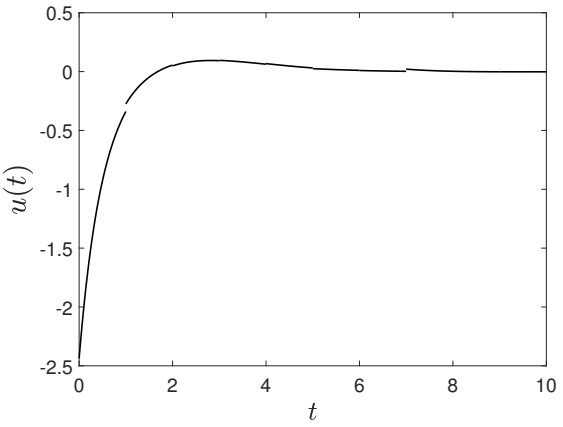

Fig. 4. Time history of the control input $\boldsymbol{u(t)}$ determined by Algorithm 1, with $\boldsymbol{\tau_M = 0.01s}$, $\boldsymbol{\tau_{rh} = 1s}$, $\boldsymbol{\nu = 6 \cdot 10^5}$, $\boldsymbol{c_1 = 0.5}$, $\boldsymbol{c_2 = 0.1}$, $\boldsymbol{\tau_{10} = \tau_{20} = 1}$ and $\boldsymbol{\gamma = 0.1}$.

(4) Implement the control input u° in the system (1b) for $\tau_\kappa - \tau_{\kappa-1}$ seconds, *i.e.* compute

$$x^\circ(t) = \varphi(t; x_c, u^\circ(\cdot)) \tag{36}$$

with $t \in [\tau_{\kappa-1}, \tau_\kappa]$, where $\varphi(t; x, u(\cdot))$ denotes the flow of the system (1b) at time t, from initial condition x and driven by the control input u.

(5) Let $x_c = x^\circ(\tau_\kappa)$, $\kappa = \kappa + 1$.

(6) **Repeat** from step (1).

A few comments about the practical implementation of the algorithm above are necessary before considering a benchmark numerical simulation. To begin with, it is worth observing that the iterations may be terminated whenever $\|x_c\|$ (which defines, via ξ_c in step (2), the intersection of the trajectory with the outer hypersphere of radius ε) is sufficiently small. In addition, in order to obtain that $\tau_\kappa = \tau_{\kappa-1} + \tau_{rh}$ for all $\kappa \in \mathbb{N}$ - namely such that the time instants at which the control law is updated coincide with the periodic pattern induced by the desired value τ_{rh} - one should select ε_ℓ sufficiently small and ν sufficiently large. This aspect is further discussed also in the numerical simulations below.

V. A BENCHMARK EXAMPLE

To illustrate and validate the theory discussed in the previous sections, the following benchmark example for infinite-horizon optimal control problems in the presence of nonlinear

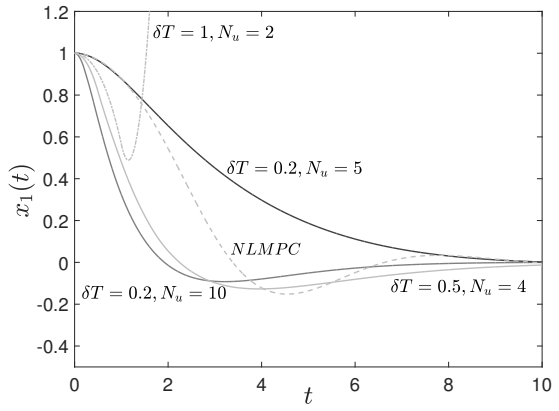

Fig. 5. Time histories of the state $\boldsymbol{x_1(t)}$ of the system (37) with $\boldsymbol{x(0) = (1, 0)}$, in closed-loop with MPC controllers for different values of the configuration parameters $\boldsymbol{\delta T}$ (sampling time) and $\boldsymbol{N_u}$ (length of the receding horizon).

dynamics is considered. In particular, the problem is borrowed from [30] and [31], where a detailed comparative analysis is carried out among several alternative techniques. Towards this end, consider the nonlinear system described by the equations

$$\dot{x}_1 = x_2\,, \quad \dot{x}_2 = x_1^3 + u\,, \tag{37}$$

with $x(t) \in \mathbb{R}^2$ and $u(t) \in \mathbb{R}$, which exhibits a cubic nonlinearity in the state variables, together with a cost functional of the form (1a), with $q(x) = x^\top x$. As implied by [20] (see also

This work is licensed under a Creative Commons Attribution 4.0 License. For more information, see https://creativecommons.org/licenses/by/4.0/

This article has been accepted for publication in IEEE Transactions on Automatic Control. This is the author's version which has not been fully edited and content may change prior to final publication. Citation information: DOI 10.1109/TAC.2022.3230764

Remark 1) the problem admits a locally $\mathcal{C}^2$ value function.

The graphs in Figures 3 and 4 depict the outcome corresponding to the strategy obtained by implementing Algorithm 1 to solve the infinite-horizon optimal control problem defined by (37) and (1a) in the *nominal* setting, *i.e.* in the absence of any noise or disturbances. The results are obtained by selecting the configurable parameters of the Algorithm 1 as $\tau_M = 0.01s$, $\tau_{rh} = 1s$, $\nu = 6 \cdot 10^5$, $c_1 = 0.5$, $c_2 = 0.1$, $\tau_{10} = \tau_{20} = 1$ and $\gamma = 0.1$. The dashed vertical lines in Figure 3, which are uniformly distributed over time, show that the selection of c_2, hence in turn of ε_ℓ at each iteration, induces the property that $\tau_\kappa - \tau_{\kappa-1} = \tau_{rh} = 1s$ for all κ. Moreover, it is worth observing that - by relying on the discussion of Remark 6, which highlights that at each execution of the steps (2)-(4) of Algorithm 1 the *entire* (infinite-horizon) optimal solution is characterized provided ε_ℓ is sufficiently small and ν is large - Algorithm 1 is capable of determining a solution with a cost lower than all the alternative techniques considered in the comparison provided in [31]. More precisely, $J(u^\circ) = 1.4828$, even with a relatively long moving window, namely with one second between two consecutive updates of the approximate policy. The proposed strategy (and its performance) is explicitly compared with control laws designed on the basis of linear and nonlinear MPC strategies (see *e.g.* [32]). In particular, within the framework of a linear (parameter-varying) MPC architecture, the dynamics (37) are linearised around the current value of the state - which is assumed constant during the prediction phase - and subsequently discretised via Euler's method, with respect to the sampling time $\delta T \in \mathbb{R}_{>0}$. To obtain a finite-dimensional characterization of the optimal control task, as it is common in this setting, it is assumed that the control action is piecewise constant during the evolution of the prediction model: this choice allows one to pose the underlying optimal control problem restricted to the moving window of length $\delta T N_u$, with $N_u \in \mathbb{N}$ denoting the prediction steps, as a static quadratic optimisation task. Figure 5 shows the time-histories of the state variable $x_1(t)$ of the system (37) for several selections of the parameters δT and N_u. In particular, the cost of the choice $(\delta T, N_u) = (0.2, 5)$ (solid black line) is equal to 1.8389. It is worth observing that for the above selection of parameters, the optimisation is performed over a receding window of one second, whereas the control action is computed every 0.2s, *i.e.* at significantly higher rate than the 1s for the control design method we propose. Furthermore, $(\delta T, N_u) = (0.2, 10)$ (solid dark gray line) induces a cost of 2.9949 , $(\delta T, N_u) = (0.5, 4)$ (solid light gray line) induces a cost of 2.1528 and, finally, $(\delta T, N_u) = (1, 2)$ (dash-dotted gray line) results in an unbounded trajectory of the closed-loop system. A similar comparison is performed also with respect to a nonlinear MPC scheme, with $\delta T = 0.2$ and $N_u = 5$, in which the optimisation problem at each step is solved via the *fmincon* command in Matlab. A quadratic *virtual* weight on the terminal state of the moving window, described by $x(t+N_u|t)^\top S x(t+N_u|t)$ with $S = 10^2 I$, is required to induce a bounded evolution to the resulting closed-loop system. The corresponding trajectory is described by the dashed gray line in Figure 5 with associated cost equal to 1.8922. The objective of the second numerical simulation is instead to assess the behaviour of Algorithm 1 in the presence of an exogenous disturbance signal affecting the dynamics (37). In particular, the disturbance is *unmatched* with the control input since it affects (linearly) the dynamics of the first state, namely $\dot{x}_1 = x_2 + w$, with $w(t)$ defined as $w(t) = 0.5$ for $t \in [0.4, 0.8]$, $w(t) = -0.5$ for $t \in [3.7, 4.2]$ and zero otherwise. The time intervals in which $w(t)$ is different from zero are visually depicted by the shaded red regions in Figures 6 and 7. It is apparent from these figures that the application of Algorithm 1, with $\tau_M = 0.01s$, $\tau_{rh} = 0.25s$, $\nu = 10^4$, $c_1 = 0.5$, $c_2 = 0.1$, $\tau_{10} = \tau_{20} = 1$ and $\gamma = 0.1$, is capable of coping with the presence of an unexpected exogenous disturbance, while still providing a control law resulting in a reasonable cost, *i.e.* $J(u^\circ) = 2.1898$.

VI. Conclusions

Infinite-horizon optimal control problems for nonlinear systems have been studied. Their intrinsically infinite-dimensional nature render this class of control problems particularly challenging to solve. The contribution of this paper has been twofold. On one hand, we have provided a *finite-dimensional* characterisation of the solution of such problems in terms of the set in which a certain function - which involves the trajectories of the associated Hamiltonian system and their sensitivity with respect to the initial condition - attains its minimum value. Then, we have shown that a suitably adapted hybrid implementation of a standard gradient-descent algorithm permits the minimisation of such functions, without requiring explicit knowledge of the flow of the Hamiltonian system, which is seldom available in practice. This result is well-suited for an *algorithmic* interpretation, which can be implemented in a receding horizon fashion. The efficacy of the resulting algorithm is demonstrated by means of a benchmark infinite-horizon nonlinear optimal control problem.

References

[1] D. A. Carlson, A. B. Haurie, and A. Leizarowitz, *Infinite horizon optimal control: deterministic and stochastic systems*. Springer Science & Business Media, 2012.

[2] L. S. Pontryagin, V. G. Boltyanskii, R. V. Gamkrelidze, and E. F. Mishchenko, *The Mathematical Theory of Optimal Processes*. John Wiley & sons, New York, 1962.

[3] R. Bellman, *Dynamic Programming*. Princeton, NJ, USA: Princeton University Press, 1957.

[4] D. P. Bertsekas, *Dynamic programming and optimal control*. Athena scientific Belmont, MA, 2005.

[5] M. Sassano and A. Astolfi, "Combining Pontryagin's principle and dynamic programming for linear and nonlinear systems," *IEEE Transactions on Automatic Control*, vol. 65, no. 12, pp. 5312–5327, 2020.

[6] A. Cernea and H. Frankowska, "A connection between the Maximum Principle and Dynamic Programming for constrained control problems," *SIAM journal on control and optimization*, vol. 44, no. 2, pp. 673–703, 2005.

[7] F. H. Clarke and R. B. Vinter, "The relationship between the Maximum Principle and Dynamic Programming," *SIAM Journal on Control and Optimization*, vol. 25, no. 5, pp. 1291–1311, 1987.

[8] P. Cannarsa, H. Frankowska, and T. Scarinci, "Second-order sensitivity relations and regularity of the value function for Mayer's problem in optimal control," *SIAM Journal on Control and Optimization*, vol. 53, no. 6, pp. 3642–3672, 2015.

[9] R. W. Beard, G. N. Saridis, and J. T. Wen, "Galerkin approximations of the generalized Hamilton-Jacobi-Bellman equation," *Automatica*, vol. 33, no. 12, pp. 2159–2177, 1997.

This work is licensed under a Creative Commons Attribution 4.0 License. For more information, see https://creativecommons.org/licenses/by/4.0/

This article has been accepted for publication in IEEE Transactions on Automatic Control. This is the author's version which has not been fully edited and content may change prior to final publication. Citation information: DOI 10.1109/TAC.2022.3230764

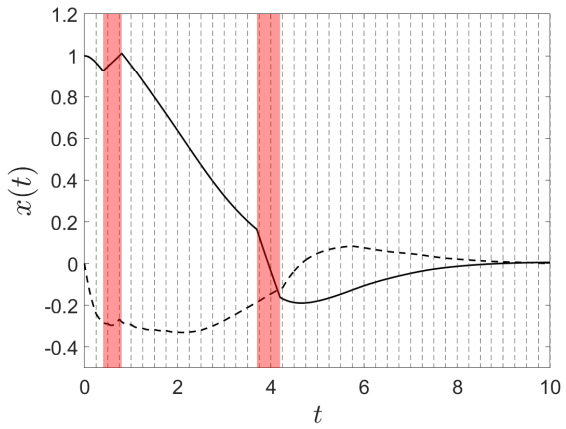

Fig. 6. Time histories of the state $\boldsymbol{x_1(t)}$ (solid line) and $\boldsymbol{x_2(t)}$ (dashed line) of system (37) with $\boldsymbol{x(0) = (1, 0)}$, in closed-loop with the control law determined by Algorithm 1, with $\boldsymbol{\tau_M = 0.01s}$, $\boldsymbol{\tau_{rh} = 0.25s}$, $\boldsymbol{\nu = 10^4}$, $\boldsymbol{c_1 = 0.5}$, $\boldsymbol{c_2 = 0.1}$, $\boldsymbol{\tau_{10} = \tau_{20} = 1}$ and $\boldsymbol{\gamma = 0.1}$, and in the presence of the exogenous signal $\boldsymbol{w(t)}$ defined as $\boldsymbol{w(t) = 0.5}$ for $\boldsymbol{t \in [0.4, 0.8]}$, $\boldsymbol{w(t) = -0.5}$ for $\boldsymbol{t \in [3.7, 4.2]}$ and zero otherwise. The red shaded areas indicate the time intervals in which the exogenous signal is nonzero.

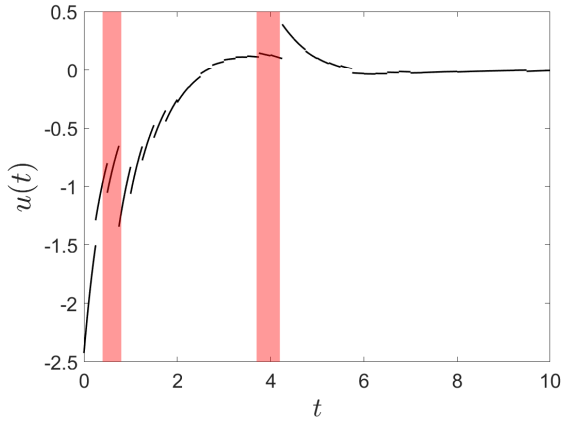

Fig. 7. Time histories of the control input $\boldsymbol{u(t)}$ determined by Algorithm 1, with $\boldsymbol{\tau_M = 0.01s}$, $\boldsymbol{\tau_{rh} = 0.25s}$, $\boldsymbol{\nu = 10^4}$, $\boldsymbol{c_1 = 0.5}$, $\boldsymbol{c_2 = 0.1}$, $\boldsymbol{\tau_{10} = \tau_{20} = 1}$ and $\boldsymbol{\gamma = 0.1}$. The red shaded areas indicate the time intervals in which the exogenous signal is nonzero.

[10] M. Bardi and I. Capuzzo-Dolcetta, *Optimal Control and Viscosity Solutions to Hamilton-Jacobi-Bellman Equations*. Birkhauser, Boston, 1997.

[11] M. G. Crandall and P. L. Lions, "Viscosity solutions of Hamilton-Jacobi equations," *Trans. Amer. Math. Soc.*, vol. 227, pp. 1–42, 1983.

[12] T. Hunt and A. J. Krener, "Improved patchy solution to the Hamilton-Jacobi-Bellman equations," in *Proc. of the 49th Conference on Decision and Control , Atlanta*, 2010.

[13] T. Çimen, "State-dependent Riccati equation (SDRE) control: A survey," *IFAC Proceedings Volumes*, vol. 41, no. 2, pp. 3761–3775, 2008.

[14] M. Sassano and A. Astolfi, "Dynamic approximate solutions of the HJ inequality and of the HJB equation for input-affine nonlinear systems," *IEEE Transactions on Automatic Control*, vol. 57, no. 10, pp. 2490–2503, 2012.

[15] M. Sassano, T. Mylvaganam, and A. Astolfi, "An algebraic approach to dynamic optimisation of nonlinear systems: a survey and some new results," *Journal of Control and Decision*, vol. 6, no. 1, pp. 1–29, 2019.

[16] N. Sakamoto and A. J. van der Schaft, "Analytical approximation methods for the stabilizing solution of the Hamilton–Jacobi equation," *IEEE Transactions on Automatic Control*, vol. 53, no. 10, pp. 2335–2350, 2008.

[17] B. Krauskopf and H. M. Osinga, "Computing invariant manifolds via the continuation of orbit segments," in *Numerical Continuation Methods for Dynamical Systems*, 2007, pp. 117–154.

[18] H. M. Osinga and J. Hauser, "The geometry of the solution set of nonlinear optimal control problems," *Journal of Dynamics and Differential Equations*, vol. 18, no. 4, pp. 881–900, 2006.

[19] R. Goebel and M. Subbotin, "Continuous time constrained linear quadratic regulator-convex duality approach," in *Proceedings of the American Control Conference*. IEEE, 2005, pp. 1401–1406.

[20] D. L. Lukes, "Optimal regulation of nonlinear dynamical systems," *SIAM Journal on Control*, vol. 7, no. 1, pp. 75–100, 1969.

[21] R. Vinter, *Optimal control*. Springer Science & Business Media, 2010.

[22] E. Al'Brekht, "On the optimal stabilization of nonlinear systems," *Journal of Applied Mathematics and Mechanics*, vol. 25, no. 5, pp. 1254–1266, 1961.

[23] D. Liberzon, *Calculus of variations and optimal control theory: a concise introduction*. Princeton University Press, 2011.

[24] C. I. Byrnes, "On the Riccati partial differential equation for nonlinear Bolza and Lagrange problems," *Journal of Mathematical Systems Estimation and Control*, vol. 8, no. 1, pp. 119–122, 1998.

[25] A. J. van der Schaft, "On a state space approach to nonlinear H_∞ control," *Systems & Control Letters*, vol. 16, no. 1, pp. 1–8, 1991.

[26] D. E. Kirk, *Optimal control theory: an introduction*. Courier Corporation, 2004.

[27] F. Borrelli, A. Bemporad, and M. Morari, *Predictive control for linear and hybrid systems*. Cambridge University Press, 2017.

[28] R. T. Rockafellar and R. J.-B. Wets, *Variational analysis*. Springer Science & Business Media, 2009, vol. 317.

[29] R. Goebel, G. Sanfelice, and A. Teel, "Hybrid dynamical systems," *IEEE Control Systems Magazine*, vol. 29, no. 2, p. 28–93, 2009.

[30] J. Markman and I. N. Katz, "An iterative algorithm for solving Hamilton–Jacobi type equations," *SIAM Journal on Scientific Computing*, vol. 22, no. 1, pp. 312–329, 2000.

[31] S. C. Beeler, H. T. Tran, and H. T. Banks, "Feedback control methodologies for nonlinear systems," *Journal of optimization theory and applications*, vol. 107, no. 1, pp. 1–33, 2000.

[32] S. Gros, M. Zanon, R. Quirynen, A. Bemporad, and M. Diehl, "From linear to nonlinear MPC: bridging the gap via the real-time iteration," *International Journal of Control*, vol. 93, no. 1, pp. 62–80, 2020.

Mario Sassano (SM, '19) was born in Rome, Italy, in 1985. He received the B.S degree in Automation Systems Engineering and the M.S degree in Systems and Control Engineering from the University of Rome "La Sapienza", Italy, in 2006 and 2008, respectively. In 2012 he was awarded a Ph.D. degree by Imperial College London, UK, where he had been a Research Assistant in the Department of Electrical and Electronic Engineering (2009-2012). Currently he is an Assistant Professor at the University of Rome "Tor Vergata", Italy. His research interests are focused on nonlinear observer design, optimal control and differential game theory with applications to mechatronical systems and output regulation for hybrid systems. He is Associate Editor of the European Journal of Control, of the IEEE CSS, EUCA Conference Editorial Boards and member of the IFAC Technical Committee on Control Design.

Thulasi Mylvaganam (SM, '21) was born in Bergen, Norway, in 1988. She received the M.Eng degree in Electrical and Electronic Engineering from Imperial College London, UK, in 2010. She completed her Ph.D. degree in 2014 in the Department of Electrical and Electronic Engineering, Imperial College London, UK, where she was a Research Associate from 2014-2016. From 2016-2017 she was a Research Fellow in the Department of Aeronautics, Imperial College London, UK, where she is currently Senior Lecturer. Her research interests include nonlinear control design, optimal control, differential game theory and distributed control with applications to multi-agent systems. She is Associate Editor for the IEEE CSS Conference Editorial Board and member of the IFAC Technical Committee on Optimal Control.

This work is licensed under a Creative Commons Attribution 4.0 License. For more information, see https://creativecommons.org/licenses/by/4.0/